Experimental and Density Functional Theoretical Investigations of Linkage Isomerism in Six-Coordinate {FeNO}⁶ Iron Porphyrins with Axial Nitrosyl and Nitro Ligands

Irina V. Novozhilova,*,† Philip Coppens,*,† Jonghyuk Lee,‡
George B. Richter-Addo,*,‡ and Kimberly A. Bagley*,§

Contribution from the Department of Chemistry, University at Buffalo, The State University of New York, Buffalo, New York 14260, Department of Chemistry and Biochemistry, University of Oklahoma, 620 Parrington Oval, Norman, Oklahoma 73019, and Department of Chemistry, State University College of New York at Buffalo, Buffalo, New York 14222

Received October 11, 2005; E-mail: ivn@buffalo.edu; coppens@buffalo.edu; grichteraddo@ou.edu; bagleyka@buffalostate.edu

Abstract: A critical component of the biological activity of NO and nitrite involves their coordination to the iron center in heme proteins. Irradiation ($330 < \lambda < 500$ nm) of the nitrosyl−nitro compound (TPP)Fe-(NO)(NO$_2$) (TPP = tetraphenylporphyrinato dianion) at 11 K results in changes in the IR spectrum associated with both nitro-to-nitrito and nitrosyl-to-isonitrosyl linkage isomerism. Only the nitro-to-nitrito linkage isomer is obtained at 200 K, indicating that the isonitrosyl linkage isomer is less stable than the nitrito linkage isomer. DFT calculations reveal two ground-state conformations of (porphine)Fe(NO)(NO$_2$) that differ in the relative axial ligand orientations (i.e., GS‖ and GS⊥). In both conformations, the FeNO group is bent (156.4° for GS‖, 159.8° for GS⊥) for this formally {FeNO}⁶ compound. Three conformations of the nitrosyl−nitrito isomer (porphine)Fe(NO)(ONO) (MSa‖, MSa⊥, and MSa$_L$) and two conformations of the isonitrosyl−nitro isomer (porphine)Fe(ON)(NO$_2$) (MSb‖ and MSb⊥) are identified, as are three conformations of the double-linkage isomer (porphine)Fe(ON)(ONO) (MSc‖, MSc⊥, MSc$_L$). Only 2 of the 10 optimized geometries contain near-linear FeNO (MSa$_L$) and FeON (MSc$_L$) bonds. The energies of the ground-state and isomeric structures increase in the order GS < MSa < MSb < MSc. Vibrational frequencies for all of the linkage isomers have been calculated, and the theoretical gas-phase absorption spectrum of (porphine)Fe(NO)-(NO$_2$) has been analyzed to obtain information on the electronic transitions responsible for the linkage isomerization. Comparison of the experimental and theoretical IR spectra does not provide evidence for the existence of a double linkage isomer of (TPP)Fe(NO)(NO$_2$).

Introduction

Nitric oxide (NO) is a small paramagnetic molecule that functions as an important biological signaling agent. NO is biosynthesized by a class of enzymes called nitric oxide synthases (NOSs).[1] The NOS enzymes contain heme as a prosthetic group, and they convert the amino acid L-arginine into NO and citrulline in two major chemical reaction steps.[2] NO binds to the heme site of NOS during turnover, and the resulting nitrosyl adduct may accumulate during catalysis to different extents depending on the isoform.[3,4] This nitrosyl adduct formally results from the reaction of the ferric heme with NO to give a product that is best described as belonging to the {FeNO}⁶ class according to the formalism of Enemark and Feltham.[5-7] Another biologically relevant heme nitrosyl of the

form {FeNO}⁶ is that of the nitrosyl nitrophorin from the blood-sucking insect *Rhodnius prolixus*.[8] In this latter example, the saliva from the insect contains the heme nitrosyl, which is secreted into the blood of the victim to result in NO release and local vasodilation.

The established biological receptor for NO is the enzyme-soluble guanylate cyclase (sGC), which contains heme as a prosthetic group.[9] NO signaling is achieved by the binding of this paramagnetic molecule to the iron center of the heme in sGC to result eventually in the production of cGMP (cyclic 3′,5′-guanosine monophosphate) from GTP (guanosine triphosphate). The nitrosyl adduct in this case is formally of the {FeNO}⁷ class, that is, an adduct of NO with ferrous heme. Typically, such {FeNO}⁷ compounds display bent FeNO geometries, whereas the corresponding {FeNO}⁶ species display linear FeNO geometries. Wieghart and co-workers have recently reported that the [Fe(NO)(cyclam-ac)]-derived compounds of

† The State University of New York.
‡ University of Oklahoma.
§ State University College of New York at Buffalo.
(1) Alderton, W. K.; Cooper, C. E.; Knowles, R. G. *Biochem. J.* **2001**, *357*, 593−615.
(2) Li, H.; Poulos, T. L. *J. Inorg. Biochem.* **2005**, *99*, 293−305.
(3) Hurshman, A. R.; Marletta, M. A. *Biochemistry* **1995**, *34*, 5627−5634.
(4) Santolini, J.; Meade, A. L.; Stuehr, D. J. *J. Biol. Chem.* **2001**, *276*, 48887−48898.
(5) Enemark, J. H.; Feltham, R. D. *Coord. Chem. Rev.* **1974**, *13*, 339−406.

(6) Feltham, R. D.; Enemark, J. H. *Top. Stereochem.* **1981**, *12*, 155−215.
(7) Westcott, B. L.; Enemark, J. H. In *Inorganic Electronic Structure and Spectroscopy*; Lever, A. B. P., Solomon, E. I., Eds.; Wiley and Sons: New York, 1999; Vol. 2 (Applications and Case Studies).
(8) Walker, F. A.; Monfort, W. R. *Adv. Inorg. Chem.* **2001**, *51*, 295−358.
(9) Boon, E. M.; Huang, S. H.; Marletta, M. A. *Nat. Chem. Biol.* **2005**, *1*, 53−59.

the form $\{FeNO\}^{6-8}$ may best be viewed as containing low-spin ferrous ion.[10] There is a growing interest in bacterial homologues of eukaryotic sGC that also bind NO,[11,12] although the in vivo functions of these bacterial proteins are yet to be fully assigned. NO is known to bind to the iron center in large number of hemeproteins such as Mb, Hb, cytochrome *c* oxidase, heme-containing nitrite reductases, and cytochrome P450.[13]

Prior to 1999, the binding of NO to heme and heme models was described solely by the N-binding mode (i.e., nitrosyl binding). The existence of O-bound (η^1-O) and side-on (η^2-NO) linkage isomers of transition metal nitrosyl complexes was discovered in the 1990s by a combination of photocrystallographic, infrared, and DSC studies and was supported by theoretical calculations.[14] The first experimental evidence that such NO linkage isomerism occurs in nitrosylmetalloporphyrins was obtained in the low-temperature (20 K) infrared study of the six-coordinate ruthenium nitrosyl porphyrins (OEP)Ru(NO)L (L = O$-i$-C$_5$H$_{11}$, SCH$_2$CF$_3$, Cl, and [py]$^+$; OEP = octaethylporphyrinato dianion).[15] These ruthenium nitrosyl porphyrins belong to the $\{RuNO\}^6$ class. Photoirradiation of the compounds resulted in changes in the infrared spectra that were associated with conversion to the isonitrosyl (η^1-O) and side-on (η^2-NO) linkage isomers as shown in eq 1.

$$\text{(1)}$$
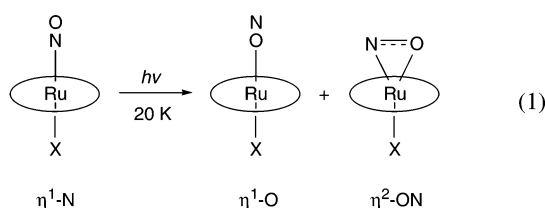
Subsequently, we showed that the low-temperature (25 K) irradiation of the five-coordinate compounds (por)Fe(NO) (por = TTP, OEP; TTP = tetratolylporphyrinato dianion) resulted in the generation of the isonitrosyls (por)Fe(η^1-ON) (eq 2).[16]

$$\text{(2)}$$
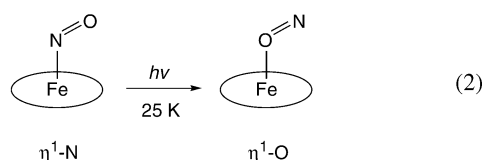
We performed, concurrently, density functional theory (DFT) calculations on the ground-state (porphine)Fe(NO) and the isonitrosyl (porphine)Fe(ON), and the calculations showed that the linkage isomer corresponded to a local minimum on the ground-state potential energy surface.[16] We showed that the calculated ground-state structure of (porphine)Fe(NO) reproduced the structural parameters determined for (OEP)Fe(NO)

by X-ray crystallography,[17,18] notably the asymmetry of the Fe$-$N(por) bond lengths and the off-axis tilt of the nitrosyl N-atom. Other workers have used theoretical calculations to reproduce these structural features of (OEP)Fe(NO).[19,20] Importantly, in our work, we also determined by theoretical calculations the optimized geometry for the isonitrosyl (porphine)Fe(ON) and showed that the bulk features were similar to those of the parent (porphine)Fe(NO). The photoinduced linkage isomers of the Ru and Fe nitrosyl porphyrins revert to the ground-state (η^1-N) nitrosyls on warming the samples. While it is generally accepted, based on the information currently available, that the ground-state structures of nitrosylmetalloporphyrins display N-binding of the NO groups to the metal centers, there is a recent report of the crystal structure of a side-on (η^2) NO group in the nitrosyl derivative of a copper-containing nitrite reductase.[21] Clearly, more new discoveries are forthcoming in the area of NO binding to biologically relevant metals.

Another nitrogen oxide of biological significance is nitrite (NO$_2^-$). Nitrite is a product of nitrate reductase activity in biological denitrification processes, and nitrite is subsequently converted to NO by the heme-containing and copper-containing nitrite reductases (NiRs).[22] It has been known for many decades that nitrite interacts with the heme iron of proteins such as myoglobin and hemoglobin, presumably through the N-atom of the nitrite.[23] The interaction of nitrite with myoglobin is an important component in the meat curing process, where the final cured meat pigment has been characterized as an iron nitrosyl porphyrin.[24] The related reactions with hemoglobin are important insofar as some studies suggest that hemoglobin is able to activate nitrite to elicit a vasodilation response and that nitrite can also oxidize the protein; these proposed roles of nitrite continue to be critically examined.[25,26]

Many coordination modes of nitrite to metals are known.[27] The predominant mode of nitrite coordination to iron porphyrins is the η^1-N mode (i.e., nitro).[28] The η^1-O binding mode is the only observed mode to date for the related Ru and Os porphyrins of the form (por)M(NO)(ONO) (M = Ru, Os),[29−32] and for the compound (TPP)Mn(ONO).[33] The published X-ray crystal structures of (por)Co(NO$_2$)-containing species contain N-bound

(10) Serres, R. G.; Grapperhaus, C. A.; Bothe, E.; Bill, E.; Weyhermüller, T.; Neese, F.; Wieghardt, K. *J. Am. Chem. Soc.* **2004**, *126*, 5138−5153.
(11) Boon, E. M.; Marletta, M. A. *J. Inorg. Biochem.* **2005**, *99*, 892−902.
(12) Nioche, P.; Berka, V.; Vipond, J.; Minton, N.; Tsai, A.-L.; Raman, C. S. *Science* **2004**, *306*, 1550−1553.
(13) Cheng, L.; Richter-Addo, G. B. In *The Porphyrin Handbook*; Guilard, R., Smith, K., Kadish, K. M., Eds.; Academic Press: New York, 2000; Vol. 4 (Biochemistry and Binding: Activation of Small Molecules), Chapter 33.
(14) Coppens, P.; Novozhilova, I.; Kovalevsky, A. *Chem. Rev.* **2002**, *102*, 861−883.
(15) Fomitchev, D. V.; Coppens, P.; Li, T.; Bagley, K. A.; Chen, L.; Richter-Addo, G. B. *Chem. Commun.* **1999**, 2013−2014.
(16) Cheng, L.; Novozhilova, I.; Kim, C.; Kovalevsky, A.; Bagley, K. A.; Coppens, P.; Richter-Addo, G. B. *J. Am. Chem. Soc.* **2000**, *122*, 7142−7143.

(17) Ellison, M. K.; Scheidt, W. R. *J. Am. Chem. Soc.* **1997**, *119*, 7404−7405.
(18) Scheidt, W. R.; Duval, H. F.; Neal, T. J.; Ellison, M. K. *J. Am. Chem. Soc.* **2000**, *122*, 4651−4659 and references therein.
(19) Wondimagegn, T.; Ghosh, A. *J. Am. Chem. Soc.* **2001**, *123*, 5680−5683.
(20) Ghosh, A.; Wondimagegn, T. *J. Am. Chem. Soc.* **2000**, *122*, 8101−8102.
(21) Tocheva, E. I.; Rosell, F. I.; Mauk, A. G.; Murphy, M. E. P. *Science* **2004**, *304*, 867−870.
(22) Wasser, I. M.; de Vries, S.; Moenne-Loccoz, P.; Schroder, I.; Karlin, K. D. *Chem. Rev.* **2002**, *102*, 1201−1234.
(23) Wanat, A.; Gdula-Argasinska, J.; Rutkowska-Zbik, D.; Witko, M.; Stochel, G.; van Eldik, R. *J. Biol. Inorg. Chem.* **2002**, *7*, 165−176 and references therein.
(24) Møller, J. K. S.; Skibsted, L. H. *Chem. Rev.* **2002**, *102*, 1167−1178.
(25) Luchsinger, B. P.; Rich, E. N.; Yan, Y.; Williams, E. M.; Stamler, J. S.; Singel, D. J. *J. Inorg. Biochem.* **2005**, *99*, 912−921.
(26) Kim-Shapiro, D. B.; Gladwin, M. T.; Patel, R. P.; Hogg, N. *J. Inorg. Biochem.* **2005**, *99*, 237−246.
(27) Hitchman, M. A.; Rowbottom, G. L. *Coord. Chem. Rev.* **1982**, *42*, 55−132.
(28) Wyllie, G. R. A.; Scheidt, W. R. *Chem. Rev.* **2002**, *102*, 1067−1089.
(29) Kadish, K. M.; Adamian, V. A.; Caemelbecke, E. V.; Tan, Z.; Tagliatesta, P.; Bianco, P.; Boschi, T.; Yi, G.-B.; Khan, M. A.; Richter-Addo, G. B. *Inorg. Chem.* **1996**, *35*, 1343−1348.
(30) Miranda, K. M.; Bu, X.; Lorkovic, I.; Ford, P. C. *Inorg. Chem.* **1997**, *36*, 4838−4848.
(31) Bohle, D. S.; Hung, C.-H.; Smith, B. D. *Inorg. Chem.* **1998**, *37*, 5798−5806.
(32) Leal, F. A.; Lorkovic, I. M.; Ford, P. C.; Lee, J.; Chen, L.; Torres, L.; Khan, M. A.; Richter-Addo, G. B. *Can. J. Chem.* **2003**, *81*, 872−881.
(33) Suslick, K. S.; Watson, R. A. *Inorg. Chem.* **1991**, *30*, 912−919.

nitro groups.[28,34] However, a nitrito-to-nitro linkage isomerization has been proposed, based on laser flash photolysis studies, to occur during the recombination of NO_2 with (TPP)Co to give the final nitro compound (TPP)Co(NO_2).[35] The reverse nitro-to-nitrito linkage isomerization is proposed for the recombination of NO_2 with (TPP)Mn to give initially (TPP)Mn(NO_2), which then decays to (TPP)Mn(ONO).[36] A recent computational study suggests that linkage isomerization is not unlikely in the nitrite adduct of cytochrome cd_1 nitrite reductase and that the availability of proton donors in the distal pocket of the protein may play a role in the potential formation of the O-bound isomer.[37]

The first significant study on the photochemical behavior of NO_2-containing transition metal complexes was done by Adell in 1955,[38] who showed that the red compound obtained from [Co(NH$_3$)$_5$NO$_2$]Cl$_2$ on prolonged exposure to sunlight is the O-bound nitrito isomer. Infrared measurements by Balzani et al.[39] and Heyns and de Waal[40] showed that the stretching bands of the N-bound NO_2, located at ∼1430 and 1315 cm^{-1}, shifted to ∼1460 and 1060 cm^{-1}, respectively, on irradiation. The new light-induced bands correspond to the O-bound NO_2 linkage isomer. Crystallographic studies of a previously irradiated single crystal of [Co$^{(III)}$(NH$_3$)$_5$NO$_2$]Cl$_2$[41] and an X-ray powder diffraction experiment[42] on the sunlight-illuminated sample of [Co$^{(III)}$(NH$_3$)$_5$NO$_2$]Br$_2$ confirmed the O-bound structure, although the geometries revealed by the two experiments are not identical.

In a recent publication,[43] we reported experimental infrared evidence and theoretical results for the photoinduced linkage isomerization in the six-coordinate {FeNO}⁶ compound (TPP)-Fe(NO)(NO_2) (TPP = tetraphenylporphyrinato dianion) involving both the NO and the NO_2 axial ligands. This low-spin compound (TPP)Fe(NO)(NO_2) belongs to the family of {FeNO}⁶ complexes. Irradiation of (TPP)Fe(NO)(NO_2) as a KBr pellet at 11 K with light from a Xe lamp results in simultaneous infrared spectral changes consistent with nitro-to-nitrito (MSa or MSc) and nitrosyl-to-isonitrosyl (MSb or MSc) conversions as shown in Scheme 1.

Although these conversions were suggested by the IR data, we could not use the data to distinguish between the singly isomerized species and the doubly isomerized species; essentially, the IR data were inconclusive as to the existence of a double linkage isomer. However, a recently completed photocrystallographic study on *cis*-[Ru(bpy) (NO)(NO_2)](PF$_6$)$_2$ confirms unambiguously that double linkage isomerization to an η^1-ONO/η^1-ON isomer occurs at 90 K in this complex.[44] Such photocrystallographic studies cannot readily be performed on

Scheme 1
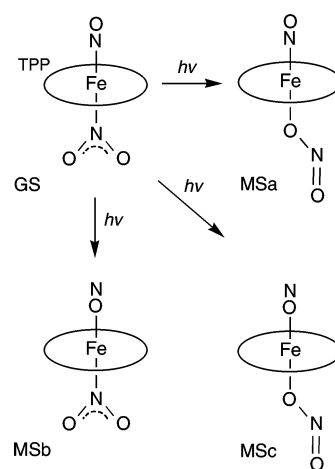
the porphyrin complexes because the deep coloration interferes with light penetration in the single crystals.

In this Article, we report the full details of the photoinduced linkage isomerization in (TPP)Fe(NO)(NO_2). Further, we have performed additional DFT calculations on the parent compound (porphine)Fe(NO)(NO_2) and determined optimized geometries for the single- and double-linkage isomers. We have computed vibrational frequencies for these isomers and analyzed the trends in band shifts upon photoisomerization. We have also determined the identities of the frontier orbitals in (porphine)Fe-(NO)(NO_2) and computed the transition energies to determine which electronic transitions and orbitals are responsible for the photoinduced linkage isomerization processes.

Experimental Section

Chemicals. The [(TPP)Fe]$_2$(μ-O) compound (TPP = 5,10,15,20-tetraphenylporphyrinato dianion) was purchased from Midcentury Chemicals. Nitric oxide (98%, Matheson Gas) was passed through KOH pellets and two cold traps (dry ice/acetone) to remove higher nitrogen oxides. ^{15}N-labeled nitric oxide (99 at. %) was purchased from Icon Isotopes and used as received. Solvents were distilled from appropriate drying agents under nitrogen just prior to use: toluene (Na) and hexane (CaH$_2$).

Preparation of (TPP)Fe(NO)(NO$_2$). (TPP)Fe(NO)(NO_2)[45] was synthesized using a published procedure[46] but with slight modifications. A Schlenk flask was charged with [(TPP)Fe]$_2$(μ-O) (0.025 g, 0.037 mmol (based on Fe)) and toluene (5 mL) under an atmosphere of prepurified nitrogen. NO gas was bubbled through the solution for 20 min, during which time the color of the reaction mixture turned from green to red-purple. Nitrogen was bubbled through the solution for <1 min to remove any unreacted NO. Hexane (20 mL) was added, and this led to the precipitation of a purple solid. The supernatant solution was discarded, and the purple solid was dried in vacuo to give (TPP)-Fe(NO)(NO_2) (0.021 g, 0.028 mmol, 76% isolated yield). IR (KBr, cm^{-1}): ν(NO) = 1874 s, ν_{asym}(NO_2) = 1461 m and ν_{sym}(NO_2) = 1298 s, δ(ONO) = 803 w. This compound slowly decomposes at room temperature to the five-coordinate (TPP)Fe(NO) derivative even under inert atmosphere. It has been shown that bubbling of inert gas through chloroform solutions of (TPP)Fe(NO)(NO_2) also results in the formation of (TPP)Fe(NO).[45]

The ^{15}N-labeled analogue, (TPP)Fe(^{15}NO)(^{15}NO$_2$), was prepared similarly using ^{15}NO gas. IR (KBr, cm^{-1}): ν(NO) = 1837 s, ν_{asym}-(NO_2) = 1431 m, ν_{sym}(NO_2) = 1278 s, δ(ONO) = 800 w.

(34) Goodwin, J.; Kurtikyan, T.; Standard, J.; Walsh, R.; Zheng, B.; Parmley, D.; Howard, J.; Green, S.; Mardyukov, A.; Przyba, D. E. *Inorg. Chem.* **2005**, *44*, 2215−2223.
(35) Seki, H.; Okada, K.; Iimura, Y.; Hoshino, M. *J. Phys. Chem. A* **1997**, *101*, 8174−8178.
(36) Hoshino, M.; Nagashima, Y.; Seki, H.; Leo, M. D.; Ford, P. C. *Inorg. Chem.* **1998**, *37*, 2464−2469.
(37) Silaghi-Dumitrescu, R. *Inorg. Chem.* **2004**, *43*, 3715−3718.
(38) Adell, B. *Z. Anorg. Allg. Chem.* **1955**, *279*, 219−224.
(39) Balzani, V.; Ballardini, R.; Sabbatini, N.; Moggi, L. *Inorg. Chem.* **1968**, *7*, 1398−1404.
(40) Heyns, A. M.; de Waal, D. *Spectrochim. Acta* **1989**, *45*, 905−909.
(41) Kubota, M.; Ohba, S. *Acta Crystallogr., Sect. B* **1992**, *48*, 627−632.
(42) Masciocchi, N.; Kolyshev, A.; Dulepov, V.; Boldyreva, E.; Sironi, A. *Inorg. Chem.* **1994**, *33*, 2579−2585.
(43) Lee, J.; Kovalevsky, A. Y.; Novozhilova, I. V.; Bagley, K. A.; Coppens, P.; Richter-Addo, G. B. *J. Am. Chem. Soc.* **2004**, *126*, 7180−7181.
(44) Kovalevsky, A. Yu.; King, G.; Bagley, K. A.; Coppens, P. *Chem.-Eur. J.* **2005**, *11*, 7254−7264.
(45) Yoshimura, T. *Inorg. Chim. Acta* **1984**, *83*, 17−21.
(46) Settin, M. F.; Fanning, J. C. *Inorg. Chem.* **1988**, *27*, 1431−1435.

Infrared Spectroscopy and Photochemistry. The methodology employed for the FT-IR experiments has been described previously.[47] Thus, FT-IR measurements were obtained on a BioRad FTS40A IR spectrometer equipped with an MCT detector. The spectral resolution was 1 cm^{-1}. The samples consisted of freshly prepared KBr pellets (approximately 1 mm thick) of the compounds, and these samples were mounted in an IR transmission cell. The cell was evacuated to $\sim$10^{-7} bar using a turbo-molecular pump. The samples were cooled to 11 K using an APD Helitran LT-3-110 optical cryostat equipped with NaCl windows and connected to a liquid N$_2$ tank, and the sample temperature was controlled to within 1 K using a Scientific Instruments 9620-R-1-1 temperature controller.

Light from a 300 W Xe arc lamp passed through a heat absorbing water filter and a 300$-$500 nm broadband filter was used for the irradiation, and the samples were mounted at 45° to both the IR beam and the irradiating light.

The sample was irradiated at various temperatures (11, 200, and 250 K), and the infrared spectra at those temperatures were recorded just prior to irradiation and then after $\sim$10 min irradiation. The decay of the metastable species was investigated by halting the irradiation, warming the sample to higher temperature (e.g., 50, 200, 250, 295 K), holding the sample at the specified higher temperature for $\sim$5 min, cooling the sample back to the initial temperature used for the irradiation experiment, and re-recording the IR spectrum.

Computational Details. All calculations were carried out in the gas phase with the Amsterdam Density Functional (ADF2004.01) program.[48-50] The calculations were performed using the nonlocal functional of Becke[51] for exchange and Lee$-$Yang$-$Parr[52] for correlation. The frozen core approximation was utilized with (1s2s2p)^{10} core on Fe, and (1s)^2 core on C, N, and O atoms. The relativistic correction was introduced with the zeroth-order regular approximation (ZORA).[53-56] A triple-ζ basis set with 4p function (TZP) was used on Fe, whereas a double-ζ quality basis set with one polarization function (DZP) was employed for all other elements. The SCF convergence criterion for the maximum element of the Fock matrix was set to 10^{-8}, while convergence criterion on the gradients was set to 4 × 10^{-4} Hartree/Å (as compared to the default setting of 10^{-2} Hartree/Å). IR frequency calculations were performed for all geometries in the gas phase. In frequency calculations, the integration accuracy was set to 8 significant digits and a "smooth freezecell" feature was applied to improve the quality of the Hessian (second derivative matrix). No scaling correction was introduced to the calculated frequencies. Time-dependent DFT (TD-DFT)[57-59] calculations of vertical excitation energies were carried out on the ground-state optimized geometry with the asymptotically correct "statistical-average-of-orbital potentials" (SAOP) using an all-electron TZP basis set on Fe and all-electron DZP basis set on all other atoms. The Davidson algorithm was used, in which the error tolerances in the square of the excitation energies and the trial-vector orthonormality

criterion were set to 10^{-8} and 10^{-10}, respectively. Graphics were done with MOLEKEL4.1 software.[60] The electron localization function (ELF) was calculated with program DGrid v2.4.[61]

Results and Discussion

X-ray Crystal Structures of (por)Fe(NO$_2$)-Containing Compounds. Scheidt and co-workers have characterized, by X-ray crystallography, a number of (por)Fe(NO)(NO$_2$) compounds.[62] The structure of the title compound (TPP)Fe(NO)-(NO$_2$) suffered from severe disorder, limiting the usefulness of the metrical data. However, accurate structural results for different crystal forms of the picket-fence derivative (TpivPP)-Fe(NO)(NO$_2$) show N-binding of both the nitrosyl and the nitro ligands to the iron center. The plane of the nitrite ion essentially bisects adjacent pairs of Fe$-$N(por) bonds in these derivatives, and the Fe atoms are displaced by 0.09$-$0.15 Å from the 24-atom mean porphyrin planes toward the nitrosyl ligands. In all heme and heme-model nitrite structures published to date, the NO$_2$ group is N-bound to the metal center. Examples include the ferrous complexes [(TpivPP)Fe(NO$_2$)]$^{-63,64}$ and [(TpivPP)Fe-(NO$_2$)(L)]$^-$ (L = CO,[65] PMS,[63] Py,[63] NO),[66] and the ferric compounds [(TpivPP)Fe(NO$_2$)$_2$]$^-$,[67] [(TpivPP)Fe(NO$_2$)-(SC$_6$F$_4$H)]$^-$,[68] and [(TpivPP)Fe(NO$_2$)(L) (L = HIm,[69] Py[69,70]). To the best of our knowledge based on the literature and an RCSB Protein Data Bank (http://www.rcsb.org/pdb/) search, only three heme proteins with bound nitrite have been characterized by X-ray crystallography, and these are the nitrite complex of reduced cytochrome cd_1 nitrite reductase from *Paracoccus pantotropha*,[71] the nitrite complex of ferric cytochrome c nitrite reductase from *Wolinella succinogenes*,[72] and the nitrite complex of ferric *E. coli* sulfite reductase hemoprotein.[73] All three protein structures also show N-binding of the NO$_2$ group to the iron centers. In fact, such N-binding of NO$_2$ groups to iron porphyrins and heme appears to dominate.[28] The only exceptions where O-binding has been established are those involving a disordered component of [(TpivPP)Fe(NO$_2$)(NO)]$^{-66}$ and that of a recently determined nitrito complex of myoglobin.[74] As mentioned earlier, the other group 8 compounds (por)M(NO)(ONO) (M = Ru,[29-31] Os[32]) possess O-bound nitrito ligands in their ground-state X-ray crystal structures.

(47) Kovalevsky, A. Y.; Bagley, K. A.; Cole, J. M.; Coppens, P. *Inorg. Chem.* **2003**, *42*, 140$-$147.
(48) te Velde, G.; Bickelhaupt, F. M.; van Gisbergen, S. J. A.; Fonseca Guerra, C.; Baerends, E. J.; Snijders, J. G.; Zeigler, T. *J. Comput. Chem.* **2001**, *22*, 931$-$967.
(49) Fonseca Guerra, C.; Snijders, J. G.; te Velde, G.; Baerends, E. J. *Theor. Chem. Acc.* **1998**, *99*, 391.
(50) Baerends, E. J.; et al. *ADF 2004.01*; SCM, Theoretical Chemistry; http://www.scm.com; Vrijie Universiteit: Amsterdam, The Netherlands, 2004.
(51) Becke, A. D. *Phys. Rev. A* **1988**, *38*, 3098.
(52) Lee, C.; Yang, W.; Parr, R. G. *Phys. Rev. B* **1988**, *37*, 785$-$789.
(53) Chang, C.; Pelissier, M.; Durand, M. *Phys. Scr.* **1986**, *34*, 394$-$404.
(54) van Lenthe, E.; Baerends, E. J.; Snijders, J. G. *J. Chem. Phys.* **1993**, *99*, 4597$-$4610.
(55) van Lenthe, E.; Baerends, E. J.; Snijders, J. G. *J. Chem. Phys.* **1994**, *101*, 9783$-$9792.
(56) van Lenthe, E.; van Leeuwen, R.; Baerends, E. J.; Snijders, J. G. *Int. J. Quantum Chem.* **1996**, *57*, 281$-$293.
(57) van Gisbergen, S. J. A.; Kootstra, F.; Schipper, P. R. T.; Gritsenko, O. V.; Snijders, J. G.; Baerends, E. J. *Phys. Rev. A* **1998**, *57*, 2556$-$2571.
(58) Jamorski, C.; Casida, M. E.; Salahub, D. R. *J. Chem. Phys.* **1996**, *104*, 5134$-$5147.
(59) Bauernschmitt, R.; Ahlrichs, R. *Chem. Phys. Lett.* **1996**, *256*, 454$-$464.

(60) Flukiger, P.; Luthi, H. P.; Portmann, S.; Weber, J. Swiss Center for Scientific Computing: Manno, Switzerland, 2000$-$2001.
(61) Kohout, M. *DGrid*, Version 2.4; Max-Planck Institute for Chemical Physics of Solids: Dresden, Germany, 2004.
(62) Ellison, M. K.; Schulz, C. E.; Scheidt, W. R. *Inorg. Chem.* **1999**, *38*, 100$-$108.
(63) Nasri, H.; Ellison, M. K.; Krebs, C.; Huynh, B. H.; Scheidt, W. R. *J. Am. Chem. Soc.* **2000**, *122*, 10795$-$10804.
(64) Nasri, H.; Wang, Y.; Huynh, B. H.; Scheidt, W. R. *J. Am. Chem. Soc.* **1991**, *113*, 717$-$719.
(65) Nasri, H.; Ellison, M. K.; Shang, M.; Schultz, C. E.; Scheidt, W. R. *Inorg. Chem.* **2004**, *43*, 2932$-$2942.
(66) Nasri, H.; Ellison, M. K.; Chen, S.; Huynh, B. H.; Scheidt, W. R. *J. Am. Chem. Soc.* **1997**, *119*, 6274$-$6283.
(67) Nasri, H.; Goodwin, J. A.; Scheidt, W. R. *Inorg. Chem.* **1990**, *29*, 185$-$191.
(68) Nasri, H.; Haller, K. J.; Wang, Y.; Huynh, B. H.; Scheidt, W. R. *Inorg. Chem.* **1992**, *31*, 3459$-$3467.
(69) Nasri, H.; Wang, Y.; Huynh, B. H.; Walker, F. A.; Scheidt, W. R. *Inorg. Chem.* **1991**, *30*, 1483$-$1489.
(70) Cheng, L.; Powell, D. R.; Khan, M. A.; Richter-Addo, G. B. *Chem. Commun.* **2000**, 2301$-$2302.
(71) Williams, P. A.; Fülöp, V.; Garman, E. F.; Saunders, N. F. W.; Ferguson, S. J.; Hajdu, J. *Nature* **1997**, *389*, 406$-$412.
(72) Einsle, O.; Messerschmidt, A.; Huber, R.; Kroneck, P. M. H.; Neese, F. *J. Am. Chem. Soc.* **2002**, *124*, 11737$-$11745.
(73) Crane, B. R.; Siegel, L. M.; Getzoff, E. D. *Biochemistry* **1997**, *36*, 12120$-$12137.
(74) Copeland, D. M.; West, A.; Soares, A.; Richter-Addo, G. B., manuscript in preparation.
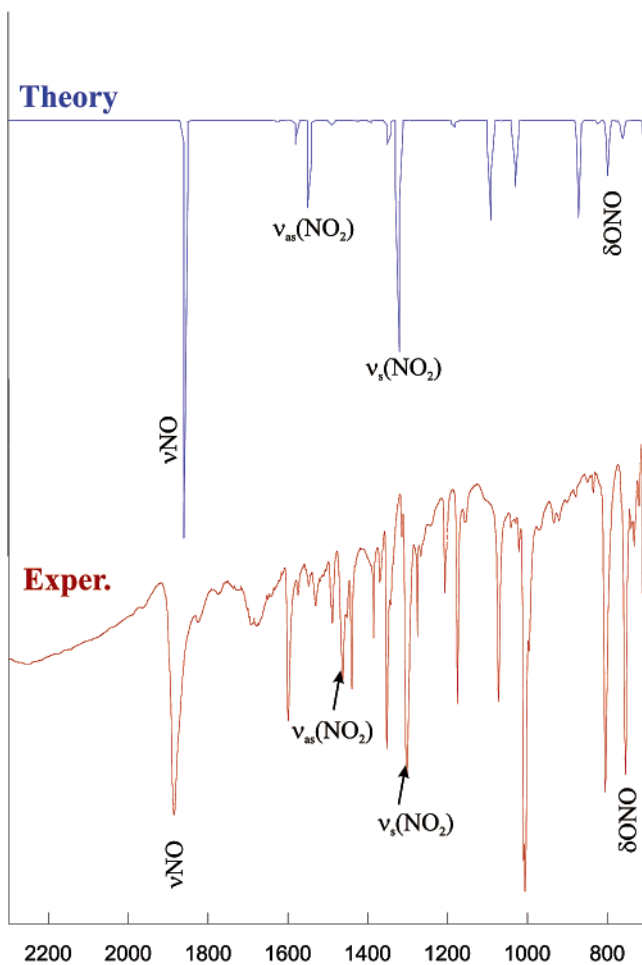
Figure 1. Comparison of the experimental ground-state IR spectrum of solid $(TPP)Fe(^{14}NO)(^{14}NO_2)$ at 11 K on KBr pellets (red) with theoretical results on $(porphine)Fe(NO)(NO_2)$ (blue) (Gaussian line profile of 16 cm^{-1} half-width) in the 700−2300 cm^{-1} frequency range.

Our DFT calculations show two ground-state conformations of $(porphine)Fe(NO)(NO_2)$, which differ primarily in the relative orientations of the axial ligand planes. In GS∥, the FeNO and FeNO$_2$ planes are mutually parallel, whereas in GS⊥ these planes are mutually perpendicular, as discussed further below.

Infrared Spectroscopy. The IR spectra of $(TPP)Fe(NO)$-(NO_2) and $(TPP)Fe(^{15}NO)(^{15}NO_2)$ (as KBr pellets) are similar to those reported previously for these compounds in CDCl$_3$[45] and as thin layers.[75] The room-temperature IR spectrum of $(TPP)Fe(NO)(NO_2)$ as a KBr pellet shows a strong ^{15}N-isotope sensitive band at 1874 cm^{-1} attributable to $\nu(NO)$. Additional ^{15}N-isotope sensitive bands at 1461, 1298, and 803 cm^{-1} are assigned to $\nu_{asym}(NO_2)$, $\nu_{sym}(NO_2)$, and $\delta(ONO)$, respectively.[27,76] These bands shift only slightly upon cooling of the sample to the photolysis temperature of 11 K, at which the $\nu(NO)$ is at 1883 cm^{-1}, and the bands due to the NO$_2$ group are at 1464, 1303, and 806 cm^{-1}. The calculated ground-state spectrum of the model compound $(porphine)Fe(NO)(NO_2)$ shows good agreement with the 11 K spectrum of $(TPP)Fe$-$(^{14}NO)(^{14}NO_2)$ as a KBr pellet, as illustrated in Figure 1.

(75) Kurtikyan, T. S.; Martirosyan, G. G.; Lorkovic, I. M.; Ford, P. C. *J. Am. Chem. Soc.* **2002**, *124*, 10124−10129.
(76) Nakamoto, K. *Infrared and Raman Spectra of Inorganic and Coordination Compounds. Part B: Applications in Coordination, Organometallic, and Bioinorganic Chemistry*, 5th ed.; John Wiley and Sons: New York, 1997; pp 48−53.

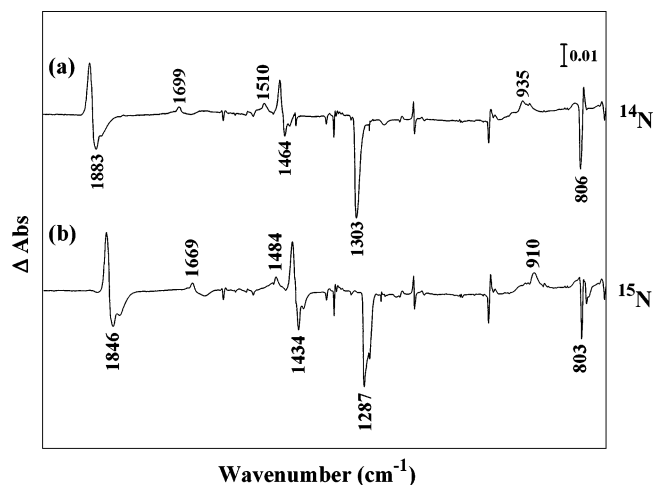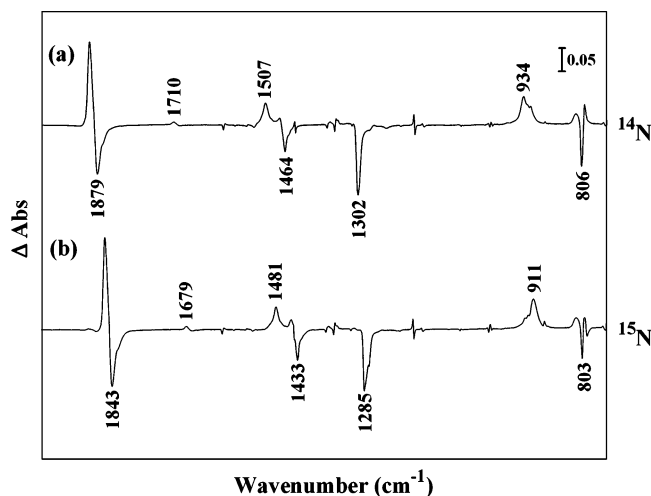**Figure 2.** Infrared difference spectra after irradiation of $(TPP)Fe(NO)$-(NO_2) at 11 K. Top, natural abundance; bottom, $(TPP)Fe(^{15}NO)(^{15}NO_2)$.

According to both experiment and theory, the symmetric NO$_2$ stretching mode is significantly more intense than the asymmetric mode. There is no noticeable difference between the calculated spectra of the GS∥ and GS⊥ conformers, suggesting that the two conformers will not be distinguishable by IR spectroscopy (see later).

Photochemistry. Irradiation at 11 K. Irradiation of (TPP)-$Fe(NO)(NO_2)$ (300 < λ < 500 nm; Xe lamp) at 11 K for 10 min results in the decrease in intensity of the infrared bands at 1464, 1303, and 806 cm^{-1} due to the nitro group (ν_{as}, ν_s, and δ_{ONO}, respectively), and the appearance of new bands at 1510 and 935 cm^{-1}. In the case of the ^{15}N-labeled compound (TPP)-$Fe(^{15}NO)(^{15}NO_2)$, photoinduced bands at 1484 and 910 cm^{-1} appeared at the expense of bands at 1434, 1287, and 803 cm^{-1} (Figure 2). The new bands are in the region associated with the ν_{as} and ν_s bands of O-bound nitrito ligands.[27,76]

In addition to the changes observed in the 1600−800 cm^{-1} region of the infrared spectra, a new but low-intensity ^{15}N-isotope sensitive band appears at 1699 cm^{-1} (Figure 2). This new band is shifted by −184 cm^{-1} from the parent nitrosyl band and is attributed to the isonitrosyl Fe−ON linkage isomer. A very small new band at 1710 cm^{-1} (not labeled) appears as a shoulder to the 1699 cm^{-1} band. This 1710 cm^{-1} band is also generated during the photolysis of five-coordinate $(TPP)Fe(NO)$ (data not shown). We therefore attribute this 1710 cm^{-1} shoulder to a derivative of a $(TPP)Fe(NO)$ impurity generated during the decomposition of $(TPP)Fe(NO)(NO_2)$ under our experimental conditions.

There is no apparent change in the IR spectrum of the photolysis product(s) when kept at 11 K over a period of 10 min, or when the sample is warmed to 50 K and kept at this temperature for 5 min before cooling to 11 K and re-recording the spectrum. We conclude that this product, after irradiation, is stable at 50 K.

Warming the sample, after photolysis, to 200 K for 10 min (and cooling back to 11 K to re-record the IR spectrum) results in the disappearance of the band at 1699 cm^{-1}; the other bands due to the newly formed nitrito group remain unchanged, indicating that the isonitrosyl group reverts to nitrosyl upon warming to 200 K.

Warming the 11 K irradiated sample to 295 K results in the loss of all of the photoinduced bands and recovery of the original
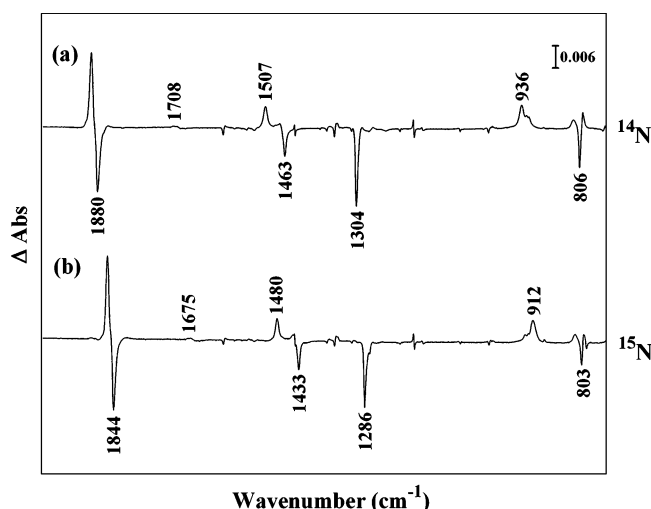
Figure 3. Difference infrared spectra after irradiation of (TPP)Fe(NO)-(NO$_2$) at 200 K. The bottom spectrum represents the changes observed for the ^{15}N-labeled analogue (TPP)Fe(^{15}NO)(^{15}NO$_2$).

Figure 4. Difference infrared spectra after irradiation of (TPP)Fe(NO)-(NO$_2$) at 250 K. The bottom spectrum represents the changes observed for the ^{15}N-labeled analogue (TPP)Fe(^{15}NO)(^{15}NO$_2$).

spectrum, collected again at 11 K, confirming that none of the linkage isomers are stable at 295 K.

Irradiation at 200 K. The difference IR spectra on 10 min irradiation at 200 K are shown in Figure 3.

The decrease in the ^{15}N-isotope sensitive bands at 1464, 1302, and 806 cm^{-1} and the appearance of new ^{15}N-isotope sensitive bands at 1507 and 934 cm^{-1} are indicative of a nitro-to-nitrito linkage isomerism, similar to that observed at 11 K, but the isonitrosyl band at 1699 cm^{-1} is absent. The very low intensity band at 1710 cm^{-1} attributed to traces of (TPP)Fe(NO) is again apparent. We note that Ford and co-workers have observed the formation of (TPP)Fe(NO) during flash photolysis of (TPP)-Fe(NO)(NO$_2$) in toluene.[77]

Irradiation at 250 K. IR spectral changes (Figure 4) on irradiation of (TPP)Fe(NO)(NO$_2$) at 250 K are similar to those at 200 K, but continuous irradiation was required to maintain adequate concentrations of the nitrito linkage isomer for IR detection, as decay to (TPP)Fe(NO)(NO$_2$) is quite fast at this temperature.

Optimized Geometries of Ground-State (Porphine)Fe-(NO)(NO$_2$) and Its Linkage Isomers. Diagrams of the ground-state and metastable state conformations of (porphine)Fe(NO)-(NO$_2$) are shown in Figure 5, together with the FeNO/NO$_2$ dihedral angles and apical displacements of the Fe atoms from the least-squares plane through the four nitrogen atoms of the porphyrin ring toward the NO ligands. The structural parameters of the optimized geometries are presented in Table 1. Side-bound η^2-NO isomers were not considered, as the experimental work provides no evidence for the formation of these species in our study.

The C_s point group was maintained during optimization of the geometries, with the exception of the MSa⊥ and MSc⊥ isomers, to which no symmetry restrictions were applied. The validity of constraining the molecules to C_s symmetry was checked through frequency calculations to ascertain that the symmetric structures correspond to stationary points on the potential energy surface. As described in the Computational Details Section, very tight optimization conditions had to be selected to locate the true minima and avoid imaginary frequencies associated with the porphyrin ring deformations. The C_s symmetry allows both the || and the ⊥ orientations of the FeNO and NO$_2$ planes.

The Ground-State Structure. In the calculated ground-state structure the nitrosyl and nitro ligands are N-bound, in accord with the X-ray structures of (por)Fe(NO)(NO$_2$) and its derivatives. In both optimized GS conformations, the FeNO group is bent, with angles of 156.4° (GS||) and 159.8° (GS⊥). Figure 6 shows a schematic of the iron environment in the calculated GS structures. The geometric parameters of the optimized structures are listed in Table 1.

In general, {FeNO}^{6} compounds display linear FeNO groups in accord with predictions from the Enemark−Feltham classification.[5−7] However, a notable exception to this linearity was observed in the related compound (OEP)Fe(NO)(*p*-C$_6$H$_4$F), in which the FeNO bond angle and the α angle are 157.4° and 9.2°, respectively,[78] a result interpreted by extended Hückel calculations as due to stabilization of the bent FeNO geometry by orbital mixing. Such mixing of the atomic orbitals is confirmed by our DFT calculations. It is of interest that, although most of the crystal forms of (TpivPP)Fe(NO)(NO$_2$) compounds display linear FeNO geometries, the related (T(*p*-OMe)PP)Fe-(NO)(NO$_2$) compound displays an FeNO bond angle of 160.2°.[62] Furthermore, Linder et al. have reported the calculated structures of several five-coordinate [(por)Fe(NO)]$^+$ compounds of the {FeNO}^{6} class and show that some of the *meso*-substituted derivatives (e.g., [(P-*meso*-(NH$_2$)$_x$)Fe(NO)]$^+$ (x = 3 or 4) may possess bent FeNO geometries.[79]

The calculated electron localization function (ELF) reveals a noncylindrical electron pairing region on the nitrosyl N-atom (Figure 7), indicative of the bending of the NO ligand and its off-axis tilting. To the best of our knowledge, this is the first theoretical result showing a "ferrous" {FeNO}^{7}-like electron pair localization on a nitrosyl N-atom in a "ferric" {FeNO}^{6} porphyrin.

(77) Lim, M. D.; Lorkovic, I. M.; Wedeking, K.; Zanella, A. W.; Works, C. F.; Massick, S. M.; Ford, P. C. *J. Am. Chem. Soc.* **2002**, *124*, 9737−9743.
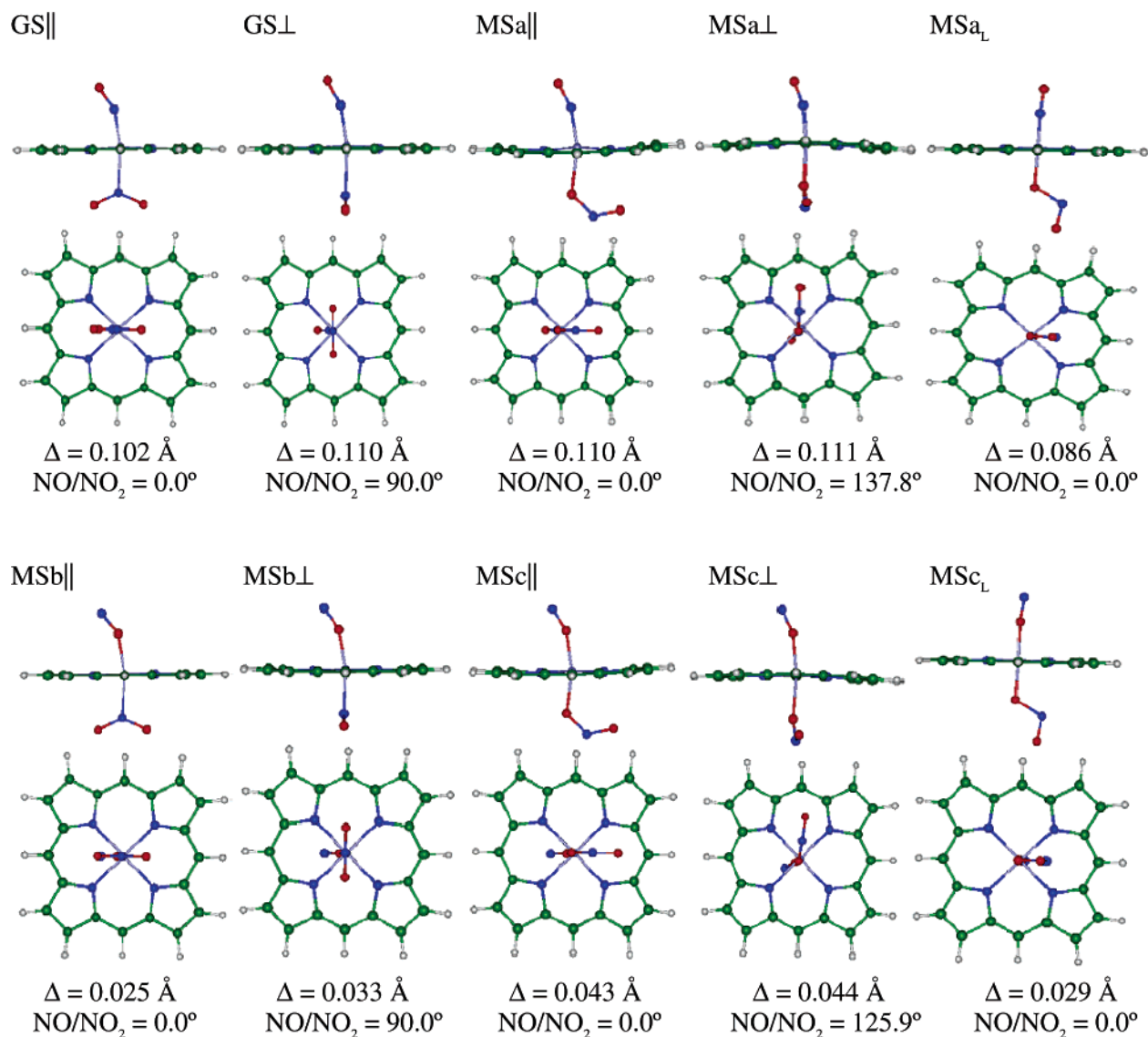
(78) Richter-Addo, G. B.; Wheeler, R. A.; Hixon, C. A.; Chen, L.; Khan, M. A.; Ellison, M. K.; Schulz, C. E.; Scheidt, W. R. *J. Am. Chem. Soc.* **2001**, *123*, 6314−6326.

(79) Linder, D. P.; Rodgers, K. R.; Banister, J.; Wyllie, G. R. A.; Ellison, M. K.; Scheidt, W. R. *J. Am. Chem. Soc.* **2004**, *126*, 14136−14148.

Figure 5. Diagrams of the optimized geometries of the ground-state and linkage isomers of (porphine)Fe(NO)(NO₂). Δ represents the apical displacement of the Fe atom from the four-nitrogen porphyrin plane toward the nitrosyl/isonitrosyl ligands. NO/NO₂ represents the dihedral angle between the FeNO (or FeON) and the NO₂ ligand planes.

Table 1. Calculated Geometries (in Å and deg) and Relative Energies (in eV) of the Ground State, Nitrito (MSa), Isonitrosyl (MSb), and Double Linkage (MSc) Isomers of (Porphine)Fe(NO)(NO₂)[a]

	nitrosyl or isonitrosyl						nitro or nitrito					
	Fe–NO	Fe–ON	N–O	∠FeNO	∠FeON	α	Fe–NO₂	Fe–ONO	β	Fe–N$_{por}$	Fe–N$_{por}$(NO)[b]	ΔE[c]
GS‖	1.675		1.152	156.4		8.7	2.021		3.4	1.992	2.008	0.000
GS⊥	1.670		1.151	159.8		8.0	2.028		2.3	1.991	2.009	+0.015
MSa‖	1.666		1.154	158.5		7.7		1.956	7.5	1.987	2.011	+0.186
MSa⊥	1.662		1.154	161.4		6.5		1.955	7.1	2.005, 1.986	2.012, 2.000	+0.197
MSa$_L$	1.647		1.149	175.4		1.7		1.869	2.8	2.002	2.007	+0.330
MSb‖		1.817	1.149		150.9	8.4	1.960		4.2	1.981	2.001	+1.356
MSb⊥		1.809	1.148		153.4	8.4	1.968		2.7	1.979	2.003	+1.376
MSc‖		1.792	1.152		154.1	7.4		1.912	7.8	1.976	2.005	+1.577
MSc⊥		1.784	1.151		157.1	6.0		1.910	7.2	1.974, 1.993	1.996, 2.007	+1.598
MSc$_L$		1.751	1.148		174.6	1.4		1.827	2.6	1.994	2.000	+1.727

[a] ‖ = axial-ligand planes coplanar; ⊥ = axial-ligand planes mutually perpendicular; MSa$_L$ and MSc$_L$ = linear NO groups. All isomers were calculated with C_s symmetry, except for MSa⊥ and MSc⊥ (see text). α and β are the deviations of the Fe-bonded axial atoms from the normal to the porphyrin plane (Figure 6). [b] The Fe–N(porphyrin) bond lengths in the direction of the NO tilt. [c] ΔE = energies of the isomers relative to GS‖.

The ELF of the Fe–NO region shows the following basins (Figure 7): three core basins C(N), C(O), and C(Fe), valence monosynaptic basins accounting for metallic free valence shell V(Fe) and for oxygen lone pairs V1(O) ∪ V2(O), and two

disynaptic basins that describe the N–O bond V(N,O) and the Fe–N$_O$ bond V(Fe,N$_O$), respectively.

The ELF topology of Fe–NO in (porphine)Fe(NO)(NO₂) closely follows the pattern similar to that found in bent Cr–
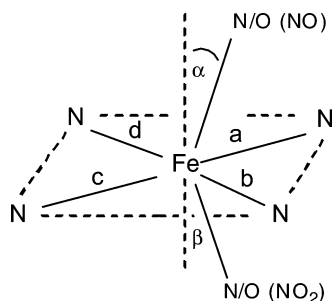
Figure 6. Schematic of the iron site in (porphine)Fe(NO)(NO₂) and its isomers. The Fe−N(por) bond lengths *a* and *b* are those in the direction of the axial ligand tilts. *a* and *b* are labeled as Fe−N$_{por}$(NO) in Table 1.
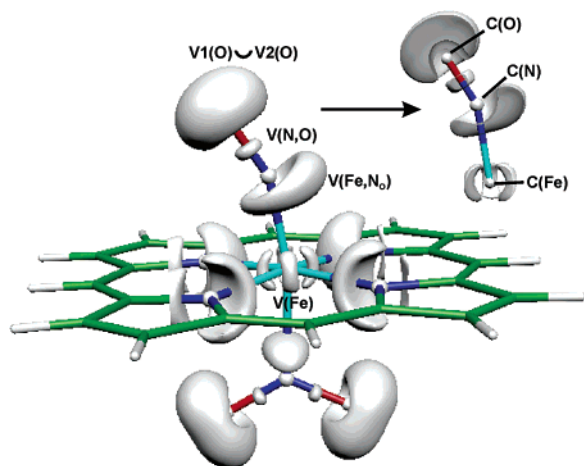

Figure 7. Electron localization function (ELF) of the (porphine)Fe(NO)-(NO₂) fragment, with a plotted isosurface value of 0.8.

CO, Cu−CO, Cr−N₂, and Cu−N₂ complexes characterized by dative bonds between metal and ligand.[80] In the formation of the dative bond, the lone pair of the ligand's atom bonding to the metal (nitrosyl N$_O$ in (porphine)Fe(NO)(NO₂)) plays a role of the disynaptic basin connecting the metal core to the ligand, whereas the π-density is transferred from the metal valence region to the ligand.[80a] It is argued that the bent structure is preferred to maximize the π-electron transfer from the metal valence density to the ligand, because this transfer is made easier when the distance between V(metal) and V(metal,ligand) (V(Fe) and V(Fe,N), respectively, in (porphine)Fe(NO)(NO₂)) is decreased. The bending is facilitated by the fact that ELF of the Fe core, C(Fe), in (porphine)Fe(NO)(NO₂) is spherically symmetric (same as in Cu/Cr−CO and Cu/Cr−N₂), as compared to repulsive cylindrical symmetry that favors linear geometry in M−N₂ and M−CO with M = Sc, Ti, V, Mn, Fe, Co, Ni.[80]

For formulation of the ELF and its applications, the reader is referred to the papers of Becke and Edgecombe,[81] Savin,[82] Kohout,[83] and Silvi.[84]

The calculated ground-state structure of (porphine)Fe(NO)-(NO₂) shows that the Fe atom is displaced by ∼0.1 Å from the

(80) (a) Pilme, J.; Silvi, B.; Alikhani, M. E. *J. Phys. Chem. A* **2003**, *107*, 4506−4514. (b) Pilme, J.; Silvi, B.; Alikhani, M. E. *J. Phys. Chem. A* **2005**, *109*, 10028−10037.
(81) Becke, A. D.; Edgecombe, K. E. *J. Chem. Phys.* **1990**, *92*, 5397−5403.
(82) (a) Savin, A.; Becke, A. D.; Flad, J.; Nesper, R.; Preuss, H.; Vonschnering, H. G. *Angew. Chem., Int. Ed. Engl.* **1991**, *30*, 409−412. (b) Savin, A.; Nesper, R.; Wengert, S.; Fässler, T. E. *Angew. Chem., Int. Ed. Engl.* **1997**, *36*, 1809−1832.
(83) (a) Kohout, M.; Savin, A. *Int. J. Quantum Chem.* **1996**, *60*, 875−882. (b) Kohout, M. *Int. J. Quantum Chem.* **2004**, *97*, 651−658.
(84) (a) Silvi, B. *J. Phys. Chem. A* **2003**, *107*, 3081−3085. (b) Poater, J.; Duran, M.; Solà, M.; Silvi, B. *Chem. Rev.* **2005**, *105*, 3911−3947.
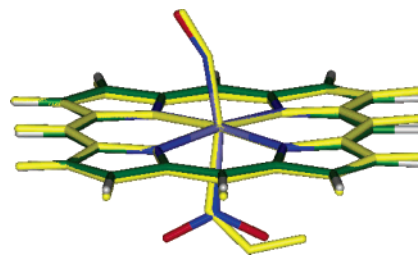

Figure 8. Superposition of the MSa∥ nitrito isomer (shown in yellow) and the ground-state GS∥ nitro isomer of (porphine)Fe(NO)(NO₂).

four-nitrogen porphyrin plane toward the NO ligand. This is in agreement with the experimental findings for the high-resolution structures of {FeNO}⁷ and {FeNO}⁶ porphyrins.[18,28,85,86] In addition, the Fe−N(por) bonds in the direction of the FeNO tilting and bending (i.e., *a* and *b* in Figure 6; Fe−N$_{por}$(NO) in Table 1) are slightly longer than the Fe−N(por) bonds that are situated away from the FeNO tilting and bending. This pattern is also observed in the related {FeNO}⁶ compound (OEP)Fe-(NO)(*p*-C₆H₄F),[78] but is opposite to that observed in five-coordinate and six-coordinate {FeNO}⁷ compounds.[18,28,85,86]

We note that the energy difference between the GS∥ and GS⊥ conformations of the model compound (porphine)Fe(NO)(NO₂) is small (0.015 eV), indicating that at room temperature both conformers may coexist. Scheidt and co-workers have determined the crystal structure of two crystalline forms of the closely related anion [(TpivPP)Fe(NO)(NO₂)]⁻ and have indeed found the ∥ and ⊥ orientations to be present in the two different crystalline forms.[66]

The Linkage Isomers. The energies of the ground-state and linkage isomer structures increase in the order GS < nitrito (MSa) < isonitrosyl (MSb) < nitrito−isonitrosyl (MSc) as detailed in Table 1. Within a given isomer, the ∥ conformer is slightly lower in energy than the ⊥ conformer (by ∼0.01−0.02 eV), and the highest energy conformations are those with linear FeNO (for MSa) or FeON (for MSc) groups. The double linkage isomer MSc$_L$ is the least stable with the energy 1.73 eV above the ground state, GS∥. The double linkage isomer MSc∥ is 1.58 eV higher in energy than GS∥, a value similar to that of 1.59 eV calculated for the nitrosyl-to-isonitrosyl linkage isomerism in the five-coordinate (porphine)Fe(NO) compound.[43] The difference in energy between the ground state and the nitrito isomers is small, similar to results obtained for an inorganic nitrito isomer.[44]

In MSa⊥, the Fe−NO plane is aligned almost along the longest Fe−N(por) bond and has an angle of 137.8° with the plane of the NO₂ group (the related angle in MSc⊥ is 125.9°). The superposition of the structures of the nitrito isomer MSa∥ onto the GS∥ is shown in Figure 8. The β tilt for the MSa∥ isomer is at 7.5° the largest among the MSa isomers. This is likely the result of increased repulsion between the terminal nitrito oxygen atom and the porphyrin macrocycle. This distortion may explain the more pronounced ruffling of the side of the porphyrin facing the terminal O-atom of the nitrito group (see Figure 8), resulting in the peripheral carbon and hydrogen atoms being displaced out of the mean porphyrin plane away from the nitrito group. Related large β tilts and ruffling

(85) Wyllie, G. R. A.; Schultz, C. E.; Scheidt, W. R. *Inorg. Chem.* **2003**, *42*, 5722−5734.
(86) Rath, S. P.; Koerner, R.; Olmstead, M. M.; Balch, A. L. *J. Am. Chem. Soc.* **2003**, *125*, 11798−11799.

Table 2. Calculated Change in the IR Vibrational Frequencies of the NO and NO₂ Ligands (in cm⁻¹) Relative to Those of the Ground State[a]

cm⁻¹	GS‖	GS⊥	MSa‖	MSa⊥	MSa$_L$	MSb‖	MSb⊥	MSc‖	MSc⊥	MSc$_L$
ν(NO)	0.0	10	−4	3	49	−58	−54	−72	−63	−25
ν_{asym}(NO₂)	0.0	−7	−17	−19	25	0	−6	−9	−10	39
ν_{sym}(NO₂)	0.0	2	−393	−395	−643	−6	−4	−421	−425	−679
δ(ONO)	0.0	0	8	6	51	2	2	−5	−6	28

[a] The vibrational frequencies are listed in Tables S3 and S4 of the Supporting Information.

distortions also occur in the isomers MSa⊥, MSc‖, and MSc⊥. It is notable that within a particular isomeric set (e.g., MSa), the α tilt generally decreases as the total energy of the conformers increases.

The N−O bond length is almost identical in all isomers (1.148−1.154 Å; Table 1), but the Mayer bond order (Table S1 in the Supporting Information) is slightly higher in the isonitrosyl isomers MSb (at 1.7) when compared to that for the nitrosyl isomers GS and MSa (at 1.5); this corresponds to a somewhat shorter bond length in the MSb isomers, with the exception of the linear isomers, the bond lengths of which are shorter than the Mayer bond order would suggest. The Fe−ON bonds in the isonitrosyl isomers (with Mayer bond orders of 0.5−0.6) are longer than the Fe−NO bonds in the nitrosyl isomers (with Mayer bond orders of 0.9−1.0), which is attributed to reduced back-donation into the antibonding π^* orbital in the O-bound isonitrosyl linkage isomers. On the other hand, the Fe−NO₂ bonds in the isonitrosyl−nitro isomers MSb are shorter (by ~0.06 Å) than the analogous bonds in the nitrosyl−nitro ground state. A similar shortening (by ~0.04 Å) of the Fe−ONO bonds in the isonitrosyl−nitrito isomers MSc relative to those of the nitrosyl isomers MSa is found, indicating that the reduced back-donation to the isonitrosyl ligands is accompanied by increased back-donation to the NO₂ ligand. This is consistent with the Fe displacement out of the porphyrin plane toward NO being smaller in the isonitrosyl isomers, in agreement with the stronger bond to the NO₂ ligand (nitro or nitrito) in the isonitrosyl isomers.

We note that the linear nitrosyl/isonitrosyl nitrito isomers (MSa$_L$ and MSc$_L$) are characterized by the least pronounced Fe axial displacement and the smallest α and β tilts. This, together with the pronounced shortening of the Fe−ONO bonds, indicates that in the linear isomers the π-accepting strengths of NO₂ and NO are much more balanced. Table S1 lists the Mayer bond orders for these groups, which reflect the calculated changes in the Fe−ligand, N−O, and O−N(O) bond lengths. The Fe−N(por) bonds are somewhat shorter in the isonitrosyl derivatives. Examination of the relevant molecular orbitals shows this to be due to an increased π-overlap in the Fe−N(por) bonds that accompanies the decrease in back-bonding to the isonitrosyl group as compared to the nitrosyl bonding (Table S2 of the Supporting Information).

Vibrational Frequencies of the Linkage Isomers. The calculated values of the vibrational frequencies of the NO and NO₂ groups of different linkage isomers relative to those of the ground-state are summarized in Table 2 and Tables S3 and S4 of the Supporting Information. The spectra constructed with Gaussian-line profiles are shown in Figure 9. Graphical representations of the vibrational modes of the NO₂ and NO groups are presented in Figures S1−S3 of the Supporting Information.

The ν(NO) bands for the nitrosyl−nitrito isomers MSa shift only very slightly (by 4−7 cm⁻¹) from those of the correspond-

ing GS isomers. There is a significant reduction in intensity of the parent symmetric stretch ν_{sym}(NO₂) upon formation of MSa, with a large shift of this band by nearly 400 cm⁻¹. There is a corresponding increase in intensity of the ν_{asym}(NO₂) band, but the δ(ONO) band decreases in intensity.

The isomers displaying linear nitrosyl and isonitrosyl ligands have the highest υ_{NO} values within their conformer sets. For example, the ν(NO) values for the MSa conformers are MSa$_L$ (1906 cm⁻¹) > MSa⊥ (1860 cm⁻¹) > MSa‖ (1853 cm⁻¹).

The calculated shift of ν(NO) from GS‖ to MSb‖ is −58 cm⁻¹, and to the corresponding double-linkage isomer MSc‖ it is −72 cm⁻¹. This is in the same direction as was previously observed for nitrosyl-to-isonitrosyl linkage isomerization,[14] but is significantly smaller than the experimental ν(NO) shift of −184 cm⁻¹ assigned to the isomerization of (TPP)Fe(NO)(NO₂). Comparison of theoretical frequencies with those detected in the IR spectra suggests that the new band detected in the 11 K irradiated sample at 935 cm⁻¹ arises from the ν_{sym}(NO₂) mode of MSa, which is also visible in the spectrum of the 200 K irradiated sample. According to the calculations, the ν_{sym}(NO₂) of MSc is 20−30 cm⁻¹ lower than that of the MSa isomers. No shift of this magnitude is observed in ν_{sym}(NO₂) on comparison of the 11 and 200 K irradiated samples. Furthermore, the spectrum of the 11 K irradiated sample shows a shoulder at 801 cm⁻¹, which according to the calculation may correspond to δ(ONO) of MSb, whereas the corresponding band of MSc is calculated to be considerably weaker. Thus, there is no evidence in the current infrared spectral data to support the existence of the double linkage isomer of (TPP)Fe(NO)(NO₂).

Finally, examination of the light-induced IR difference spectra at 11, 200, and 250 K (Figures 2, 3, and 4) shows a large differential feature at ca. 1899/1883 cm⁻¹. Such a differential feature is consistent with the possibility that the ν(NO) band shifts to slightly higher frequency upon formation of MSa. Calculation shows that formation of two of the MSa states (MSa⊥ and MSaL) gives rise to an upshift in the ν(NO) band, while formation of the MSa‖ gives rise to a downshift in the ν(NO) band. It is, therefore, tempting to conclude that it is formation of either the MSa⊥ or the MSaL state that is detected in the IR experiment. However, comparison of the calculated and experimentally observed ν_{asym}(NO₂), ν_{sym}(NO₂), and δ-(ONO) shows that the frequency shifts are not consistent with such a claim. A differential feature associated with ν(NO) bands upon formation of isonitrosyl linkage isomers has also been observed by us in both the five-coordinate (OEP)Fe(¹⁴NO) and (OEP)Fe(¹⁵NO) systems and attributed to band profile changes in the ν(NO) band upon irradiation.[16]

Insights into the Linkage Isomerism. The mechanism of the photoinduced linkage isomerism in small transition-metal nitrosyl complexes, such as sodium nitroprusside (SNP), is an electronic transition from a metal-based orbital to a mainly π^*(NO) orbital followed by radiationless transition to the ground-state potential energy surface and relaxation into a local

GS‖ and GS⊥

MSb‖ (MSb⊥ similar)

MSa‖ (MSa⊥ similar)

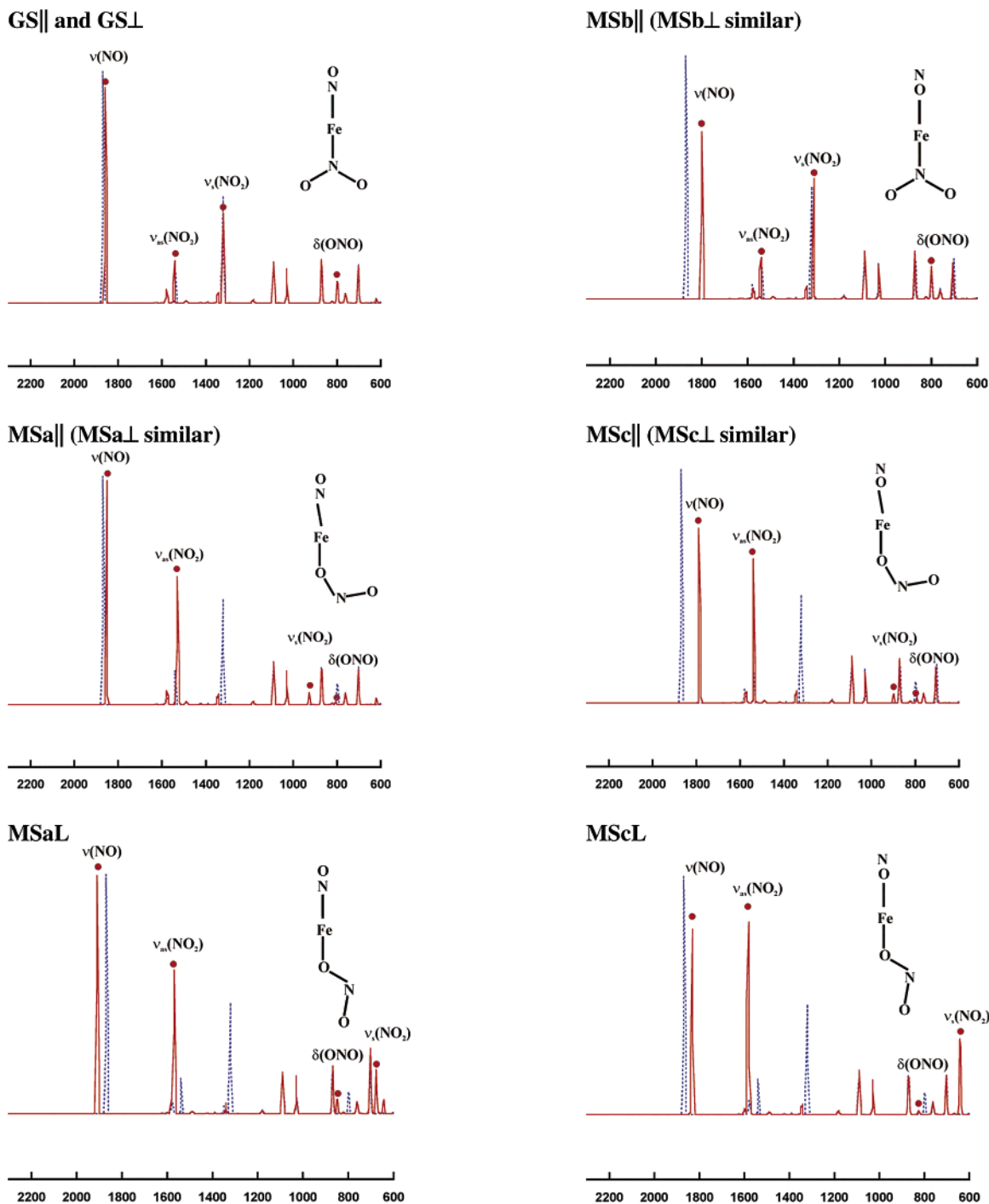**MSc‖ (MSc⊥ similar)**

MSaL

MScL

Figure 9. Calculated IR spectra of the linkage isomers of (porphine)Fe(NO)(NO₂) in the 600−2300 cm⁻¹ frequency range, with a Gaussian line profile of 16 cm⁻¹ half-width. The ground-state spectrum is shown as dotted blue lines. The NO and NO₂ peaks are marked with red dots.

minimum on that surface.[87−91] On the other hand, the nitro−nitrito linkage photoisomerization in small transition-metal complexes has been attributed to ligand (NO₂⁻) to metal charge-transfer excitation.[39,92,93]

In the case of (porphine)Fe(NO)(NO₂), the situation is considerably more complex as the UV−vis part of the spectrum is dominated by $\pi-\pi^*$ transitions of the porphine dianion (Table S5 of the Supporting Information). The frontier molecular orbitals of the ground-state (porphine)Fe(NO)(NO₂) from TD-DFT/SAOP calculations are shown in Figure 10, whereas its theoretical gas-phase absorption spectrum in the 200 < λ < 1000 nm region is reproduced in Figure 11.

(87) Delley, B.; Schefer, J.; Woike, Th. *J. Chem. Phys.* **1997**, *107*, 10067−10074.
(88) Schefer, J.; Woike, Th.; Imlau, M.; Delley, B. *Eur. Phys. J. B* **1998**, *3*, 349−352.
(89) Boulet, P.; Chermette, H.; Weber, J. *Inorg. Chem.* **2001**, *40*, 7032−7039.
(90) Boulet, P.; Buchs, M.; Chermette, H.; Daul, C.; Gilardoni, F.; Rogemond, F.; Schläpfer, C. W.; Weber, J. *J. Phys. Chem. A* **2001**, *105*, 8991−8998.
(91) Boulet, P.; Buchs, M.; Chermette, H.; Daul, C.; Furet, E.; Gilardoni, F.; Rogemond, F.; Schläpfer, C. W.; Weber, J. *J. Phys. Chem. A* **2001**, *105*, 8999−9003.

(92) Scandola, F.; Bartocci, C.; Scandola, M. A. *J. Phys. Chem.* **1974**, *78*, 572−575.
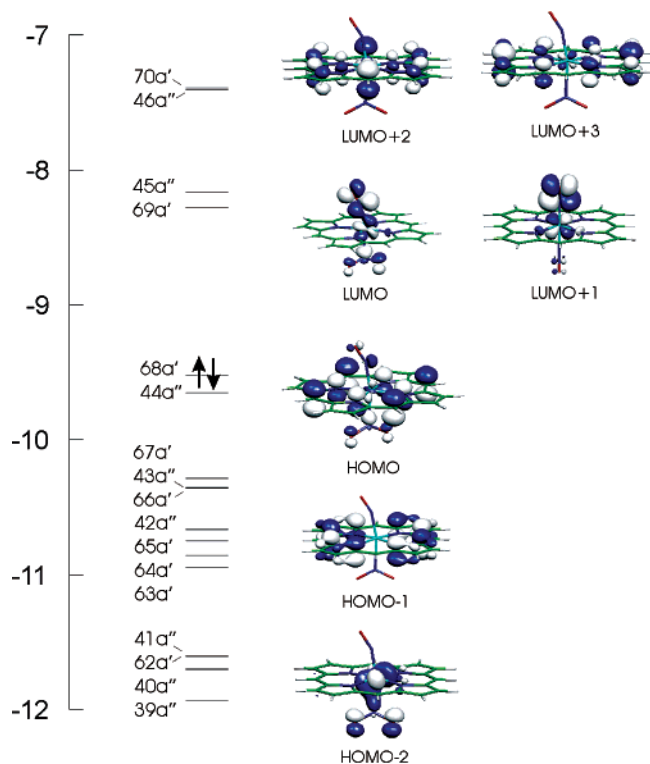(93) DeLeo, M. A.; Ford, P. C. *Coord. Chem. Rev.* **2000**, *208*, 47−59.

Figure 10. Energy level diagram of (porphine)Fe(NO)(NO₂) in the ground state from the TDDFT/SAOP calculations (using C_s symmetry). The occupation of the HOMO orbital is indicated by two arrows.
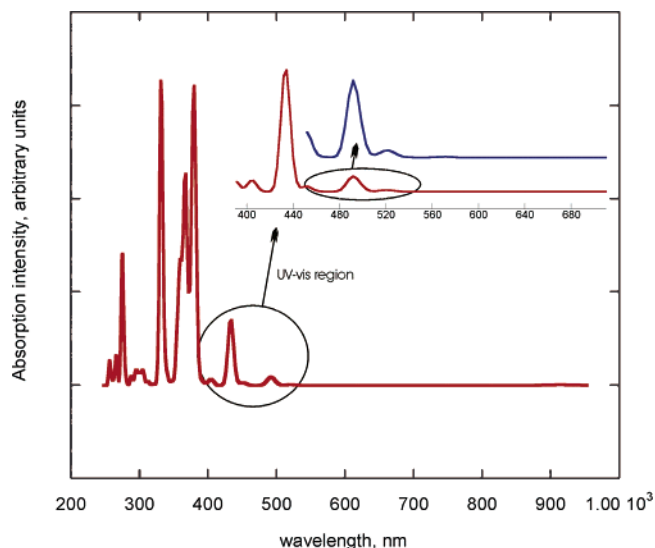

Figure 11. Calculated gas-phase absorption spectrum of (porphine)Fe-(NO)(NO₂), with a Gaussian line profile of 500 nm half-width. The detailed UV−vis region is shown as an inset with the low-energy part enlarged in blue.

The UV−vis part of the spectrum in the inset of Figure 11 shows a characteristic Soret band near 433 nm, in excellent agreement with the experimental values for the tetraarylporphyrin compounds (TPP)Fe(NO)(NO₂) (433 nm in CHCl₃;[45] 431 in CH₂Cl₂[62]), (T(*p*-OMe)PP)Fe(NO)(NO₂) (437 nm in C₆H₅-Cl),[62] and (TpivPP)Fe(NO)(NO₂) (433 nm in toluene).[62] According to the TDDFT/SAOP calculations, the intense Soret band in the near UV arises from excitations from HOMO−2 to almost degenerate LUMO+2 and LUMO+3 Gouterman π^* orbitals: these intense transitions result in 12A″ and 13A′ states in (porphine)Fe(NO)(NO₂) (Table S5 of the Supporting Infor-

mation). Such transitions to Gouterman orbitals in Mg, Zn, and Ni porphyrin and porphyrazine complexes have been investigated extensively by Baerends et al.[94]

As the linkage isomerization is induced with light from a Xe arc lamp that emits in the 300−500 nm region, we will concentrate on the 300−500 nm region in our analysis. Altogether 52 transitions were calculated in this range (Table S5), but only those involving orbitals on Fe atom, NO and NO₂ ligands, and N(por) of the porphyrin ring are relevant for the discussion of the isomerization mechanism. Analyses of Table S5, Figure 10, and Figure S4 show that there are several transitions involving the metal d-orbitals and the NO and NO₂ ligands. The relevant d_{Fe}-π^*(NO) transitions, which according to the earlier studies[87,88] are involved in the nitrosyl to isonitrosyl isomerization, lie in the low-energy part of the spectrum, at 463 nm (to state 8A″) and 452 nm (to state 9A′). The transition from nitro-centered orbital to the metal, which according to the literature is involved in the nitro-to-nitrito isomerization,[39,92] also occurs in this spectral range (Table S5). Thus, the calculations confirm that both nitrosyl and nitro isomerizations can be induced by light of 300−500 nm. In support of this conclusion is the observation by Ford and co-workers[77] that flash photolysis of (TPP)Fe(NO)(NO₂) in toluene at 298 K results in competitive dissociation of NO and NO₂ to give (TPP)Fe(NO₂) and (TPP)Fe(NO).

In the photolysis experiments, we found that the infrared bands of the parent (TPP)Fe(NO)(NO₂) were restored upon warming the photolyzed sample back to room temperature, indicating reversibility of the linkage isomerism. Calculations of the activation energy barriers are thus required for a complete understanding of the thermal stability and decay of the linkage isomers. This involves investigation of several reaction coordinates, such as mutual rotation and bending of both the NO and the NO₂ ligands on the multidimensional ground-state potential energy surface, and may be subjected to a further study.

Conclusions

We have shown that the low-temperature photolysis of the six-coordinate {FeNO}⁶ compound (TPP)Fe(NO)(NO₂) results in linkage isomerization involving nitro-to-nitrito and nitrosyl-to-isonitrosyl conversions. Using DFT calculations, we have identified two ground-state conformations, GS‖ and GS⊥, which differ in the relative axial ligand orientations, and three single-linkage isomers resulting from the nitro-to-nitrito conversion (MSa). Two single-linkage isomers with isonitrosyl ligands (MSb), and three double-linkage isomers with isonitrosyl and nitrito ligands (MSc), also correspond to local minima on the ground-state potential energy surface. The energies of these isomers increase in the order GS < MSa < MSb < MSc. This is consistent with the experimental finding that the nitrito linkage isomers are more stable than the isonitrosyl linkage isomers. Further, the isomers with mutually parallel axial ligand planes are slightly more stable than the corresponding conformers with perpendicular axial ligand planes, but the energy difference is small, suggesting that GS‖ and GS⊥ may coexist at room temperature. With the exception of the two linear linkage isomers, all of the species contain bent FeNO bonds that exhibit off-axis tilting of the bonded atom (O or N) in the direction of

(94) Baerends, E. J.; Ricciardi, G.; Rosa, A.; van Gisbergen, S. J. A. *Coord. Chem. Rev.* **2002**, *230*, 5−27.

the longer Fe—N(por) bonds. We also find that the conformers with linear FeNO groups (and smallest off-axis tilts) are highest in energy within a given isomer, a novel finding for this {FeNO}^{6} compound class. In general, the Fe—(ON) bonds are longer in the isonitrosyl isomers, whereas the Fe—(NO$_2$) bonds are shorter. This is attributed to the reduced back-donation to the isonitrosyl ligand and leads to a reduction of the displacement of the iron atom from the porphyrin plane toward the NO ligand.

Vibrational frequency calculations were performed on all of the linkage isomers. Within an isomeric set (i.e., nitrosyl—nitrito or isonitrosyl—nitro or isonitrosyl—nitrito), the v_{NO} varies as a function of linearity of the FeNO groups and the relative axial ligand orientations. The computed energy difference between the lowest-energy ground state and the lowest-energy double-linkage isomer is 1.58 eV, which is comparable to the 1.59 eV computed previously for the experimentally observed (por)Fe-(NO)-to-(por)Fe(ON) linkage isomerism. However, the experimental IR spectra in the current work do not provide evidence for the existence of a double linkage isomer of (TPP)Fe(NO)-(NO$_2$).

The results of the current study suggest that the nature of interactions of NO and nitrite with iron porphyrins in biological systems may be more diverse than commonly assumed with the possibility of one or more linkage isomers playing a role in association of NO and NO$_2$ groups with biologically relevant iron, or in dissociation processes involving these groups. The fact that these linkage isomers are photochemically accessible indicates that these isomers should be considered in interpretations of experiments involving photolysis of nitrosyl hemes or their nitrite derivatives.

Supporting Information Available: Mayer bond orders for Fe—NO/ON, Fe—NO$_2$/ONO, N—O, and O—N—O bonds; changes in the overlap population $\Delta(GS\|-MSb\|)$ of Fe, NO, and NO$_2$ fragments in selected molecular orbitals; experimental and theoretical ground- and metastable-state IR values of NO and NO$_2$ vibrations; TDDFT singlet—singlet excitations in $300 < \lambda < 930$ nm region; graphical representations of NO and NO$_2$ IR vibrations; graphical representations of selected molecular orbitals from TDDFT calculation; complete ref 50. This material is available free of charge via the Internet at http://pubs.acs.org.

JA0567891